IADIS International Journal on Computer Science and Information Systems
Vol. 6, No.1, pp. 1-13
ISSN: 1646-3692

EFFICIENT PIXEL BINNING OF PHOTOGRAPHS

Thilo Bauer, *bluewater multimedia concepts, Heimerzheimer Str. 2, D-53332 Bornheim, Germany*
tbauer@astro.bwmc.net

ABSTRACT

Pixel binning is a well-known method to reduce the storage capacity of digital images. There remains the question, however, whether binned images obtain an increase of signal or signal-to-noise ratio. Experiments with photographs of point light sources and extended light sources are presented to demonstrate (a) the effect of increase of signal and (b) the success of pixel binning. The work presents a method to compute the signal-to-noise ratio for the binning task. On-chip binning is provided by some hardware devices. On-chip binning will introduce a certain complexity to the calibration of the device and to the derivation of errors obtained from photometry. Electronic imaging and photography are based on physical constraints. It is shown, that binning does not violate the physical law of conservation of energy. Binning will provide averaged pixels at lowered dimension and resolution of the image. Binning does not improve the signal-to-noise ratio or the susceptibility of the device.

KEYWORDS

Binning, linear image processing, analysis, photometry

1. INTRODUCTION

Imaging and photometry of any scene are a challenge, where the illumination level falls down to the order of the level of detector noise. This is the case in certain fields of science, like the astronomy or microscopy. Typical examples are deep sky imaging and photometry of faint stars or galaxies or measuring photo luminescence in microscopy. The methods of astronomical imaging define a typical task of image calibration and data reduction (Mackay, 1986 and Berry & Burnell, 2006). Almost every astronomical observatory uses individually developed detector hardware with the telescopes. This leads to dedicated processing pipeline established to calibrate the real detector (Blakeslee, 2003).

Pixel binning is a simple arithmetic image transformation: All pixels from the local pixel group of N×N are averaged (sum and division by N*N) and stored as one single pixel in a new image with a dimension lowered by N. Therefore, 1×1 binning represents the image itself, as binning 1×1 is the identity transformation. 2×2 pixel binning averages a matrix of 4

neighboring pixel lying in the consecutive row indices *r* and column indices *c*. 3×3 pixel averages a matrix of 9 pixel values, and so forth. The image shrinks in resolution by a factor defined by the dimension of the bin. Binning is provided with certain imagers based on a hardware procedure to bin the recorded pixel before the storage of the image. This is called on-chip binning (Mullikin, 1994 and Fellers & Davidson, 2010). Binning N×N reduces storage capacity by a factor N^2 compared to the original resolution. If blur is obtained from imaging, pixel binning applies to reduce the spatial resolution and average pixel values. Pixel binning is also claimed to yield an increase of the signal-to-noise ratio (Howell, 2006 and Fellers & Davidson, 2010).

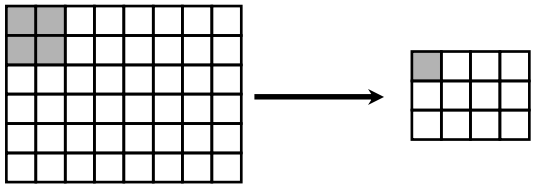

Figure 1. The principle of N×N binning: A matrix of N×N pixel is transformed into one single pixel.

2. FLUX AND NOISE

An image shall be regarded as a set of numbers *I(x)*, which are the measured pixel intensity values at the two-dimensional coordinate *x*. There are not only intensities stored with the pixel values, but also constraints from geometry and the physics of the device. The incoming flux of the light will cause electrons created within the silicon and collected over time. The pixel intensities *I(x,t)* therefore represent a flux from the source at time *t*. The electron current from the chip is amplified and digitized by the electronics. This yields a certain conversion factor g_{PC} between the original photo electrons and the digital numbers obtained. The relation between the measured photo current $N_{PE}(x,t)$ and the number $N_Q(x,t)$ of photo events detected is given by a certain quantum efficiency q_v at frequency *v* (Mullikin, 1994).

$$I(x,t) = g_{PC}\, N_{PE}(x,t) = g_{PC}\, q_v\, N_Q(x,t) \quad \text{Eq. 1a}$$

$$I(x) = g_{PC}\, N_{PE}(x) = g_{PC}\, q_v\, N_Q(x) \quad \text{with} \quad N_Q(x) = \int_{\Delta t} N_Q(x,t)\, dt \quad \text{Eq. 1b}$$

The flux may vary over over time *t*, i.e. a variable star to be measured in the astronomy or a variation of photo luminescence in microscopy. Within the exposure time Δt a camera is unable to detect variations and integrates the flux over time (equation 1b). The numbers *I(x)* are not necessarily positive. If analog-digital converters provide a positive number range only, negative numbers are often avoided by a certain electronic bias, which is corrected by a calibration and subtraction to obtain the effective values *I(x)*. For the real detector the total current is given by several statistics of error sources, which are independent or not. These are at least a number of „real“ photo electrons $N_{PE}(x)$ measured from the flux and a number of electrons $N_{Dark}(x)$ which are accidentally detected. These accidentally detected electrons are created by the thermal physics of the silicon, therefore called dark current. If the number of

photo electrons and dark electrons are statistically independent (which has to be proven with the real device), the dark signal is additive and can be compensated by a subtraction of $N_{Dark}(x)$.

$$I(x) = g_{PC} \left(N_{PE}(x) + N_{Dark}(x) \right)$$
Eq. 2

Using a property of the Poisson distribution, there are further relations between the expectation value of the photo electrons $\langle N_{PE}(x) \rangle$ and variance $Var(N_{PE}(x))$ and the corresponding expectation value $\langle I(x) \rangle$ and standard deviation σ_I (Mullikin, 1994):

$$Var(N_{PE}(x)) = \langle N_{PE}(x) \rangle = 1/g_{PC} \langle I(x) \rangle, \qquad Var(I(x)) = \sigma_I^2 = g_{PC}^2 \, Var(N_{PE}(x))$$
Eq. 3

This allows to compute the electron conversion factor g_{PC} from the digital numbers $I(x)$ and noise analysis from a stationary signal. Finally the number N_{PE} of the photo electrons detected can be obtained (Mullikin, 1994 and Berry & Burnell, 2006). With the real detector the physical relation between the energy and the number of photo events is determined by

$$E = h\, v, \qquad \sum^{n} q_v E_n = E\, q_v N_Q(x) \sim N_{PE}(x)$$
Eq. 4

where E is the energy, h is Planck's constant and v the frequency of the light (Planck, 1901). E_n is the energy of a single photo quant with index n. In the case of monochromatic light E_n is a constant. The photo current $N_{PE}(x)$ obtained from the number n of the individual photo electrons is proportional to the total energy E of the photo events detected. The polychromatic case yields the probability to detect a photo event as a multiplication of the spectral distribution of flux emitted by the spectral sensitivity of the detector, which is given by the quantum efficiency q_v. With incoherence (incoherent light, i.e. thermal light source), the single photo events are statistically independent. The expectation value $\langle N_{PE}(x) \rangle$ is proportional to the expectation value of the wavelength-weighted energy obtained from the photo flux.

$$g_{PC} \langle \sum^{n} q_v E_n \rangle = g_{PC} N_Q \langle q_v E_n \rangle \sim \langle N_{PE}(x) \rangle$$
Eq. 5

There are further noise sources identified with the image (Gilliland, 1992). One of these effects is the individual photo response with every pixel. It is a non-additive noise (Gilliland, 1992) caused by and composed of several physical constraints like vignetting, and solid-state physics. Therefore, the image of a flat illumination will not yield evenly distributed pixel intensities. This is compensated by the recording of an evenly illuminated field (flat) field and a further arithmetic division by the normalized image of the flat field. The concept of this calibration procedure is called flatfield (or flatfielding). If linear processing and analysis is required, the real detector may be found with certain non-linearities. In this case, g_{PC} might be a non-linear function of N_Q. The inverse of g_{PC} shall linearize the numbers $I(x)$ before the image analysis.

3. EXPERIMENTAL BINNING

An experiment has been done to illustrate the effect of an improvement of the signal-to-noise ratio and the success of binning. The famous Dumbell Nebula (Messier 27, NGC 6853) has been recorded using an astronomical telescope of 20 cm diameter and about 1200 mm focal length. The exposure time was 30 seconds. The camera was a Canon EOS 40D. The set of raw frames consists of 200 individual frames taken at full resolution (1944×1296 raw pixel from a RGB Bayer matrix, no pixel interpolation was applied). From this set of frames the first 4 raw frames have been selected which did not show guiding errors (instabilities of the telescope mount) and defects caused by the atmosphere (scintillation, seeing). The image calibration was performed by a dark signal subtraction and flatfield division (see section 2), both obtained from the average of 200 single raw frames. This to reduce noise sources introduced by the calibration. Figure 2a shows a portion of the single image. Figure 2b shows the result of co-adding four images in such a way, that they have been corrected for image motion (shift-and-add). Figure 2c shows the same image as 2a, except 2×2 binning was applied. The offsets (sky background) have been carefully evaluated by computation of the mean value of the sky background and subtracted. Then the image results have been normalized to show the same intensity range. Therefore, the co-added image is divided by 4. The standard deviation of the background illumination yielded 49.70 DU (digital units) for the single frame, 32.83 DU for the co-added exposure and 28.34 DU for the binned result of the single frame. Obviously, the co-added exposure 2b and the binned single frame 2c yielded almost the same peak signal-to-noise ratio after the normalization.

From a visual inspection the binned sample 2c looks smoother than figure 2a. (The printing and display process of the paper might suggest 2a and 2c look perfectly the same, however). The single raw image and the binned result contain almost the same amount of stars, perhaps with statistical drop of a few suggested stars and others more clearly visible. The features of the nebula seem to look almost the same. Figure 2b shows the result of a 4 times larger exposure time, which is obtained by the sum of four images. The surface brightness of the nebula looks less noisy and faint details are visible in figure 2b. From the visual inspection, collecting information of four neighboring pixels does not seem to provide the same result as collecting four independent measures at some pixel locations. There are slight indications to have found more stars and details from the nebula with the co-added long-exposure 2b. Will this be confirmed by further analysis?

A search of the local maxima above 3 sigma of standard deviation has been applied to the pictures. This represents a probability of more than 99% to detect a peak above noise. A threshold at different minimum distances of the peaks has been set. The minimum distance of peaks is divided by two for the binned results at lower resolution. Therefore, stars with a distance of 2 pixel at full resolution cannot be detected as two peaks from the binned images. Due to the correction of image motion, the co-added image has left a border, where the number of images added is smaller than the total number of frames. This would result in a different probability to detect a peak due to a smaller amount of intensities added, which also yields more noise. Therefore, a border of 30 pix has been excluded from the search, which is larger than the maximum value of image motion. A rectangular area around the nebula has also been excluded from the star search. This avoids detection of wrong peaks due to the intensity offset of the bright nebula. The projected region of interest was set identical to all three images, however. The analysis has been applied to the binned single frame, the co-added

frame at full resolution and a binned version of the co-added frame. Table 1 presents the amount of stars obtained for the whole image.

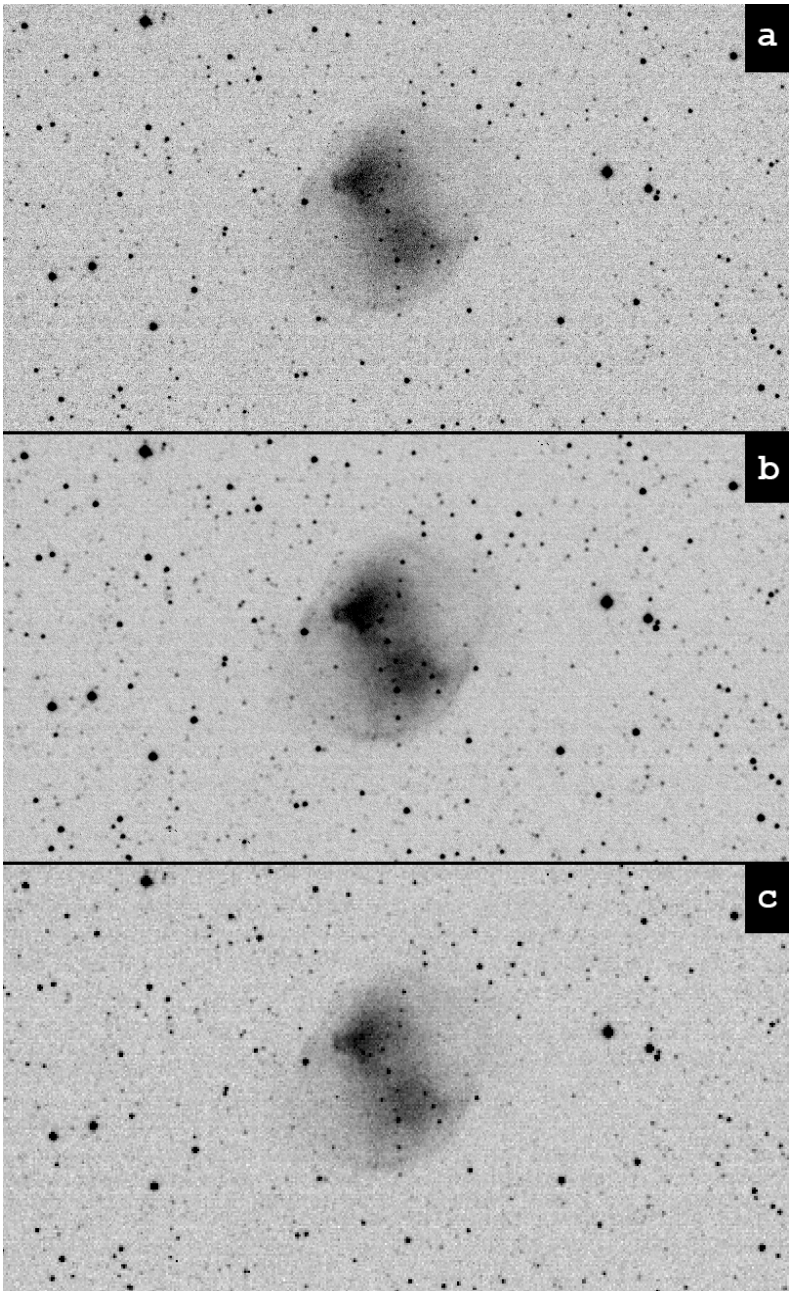

Figure 2. Dumbell Nebula (part of picture): a) raw frame, b) four co-added raw frames and c) result of 2×2 binning of a).

A major problem found with the single exposure 2a was as a certain amount of hot pixel defects detected as „stars“. Its analysis is rejected, therefore. It seems more interesting to compare the binned short-exposure with the long-exposure instead. This to see, whether binning yields a gain of signal versus noise. A careful evaluation of the binned single image yielded a certain amount of hot pixels accidentally detected, too. Therefore the amount of stars is slightly overestimated in the binned single image. At some minimum distances, the binned sample provides more stars and compared to the co-added image, then drops below the result of the co-added image at a minimum distance of 3 pixel. A larger exposure time, represented by the co-added frame, is expected to yield better photo electron statistics. The analysis yielded a significant smaller amount of stars, if 2×2 binning was applied to the co-added image. In spite of larger standard deviation, the co-added image yields up to 11% more stars at full resolution. Equality between the binned single exposure and the co-added frame is uncertain due to noise properties of the detector (pixel defects, hot pixel). With a certain probability, the amount of stars found in the co-added image is larger (marginal, however). The overall result remains contradictory and will not meet expectations, if a gain in SNR is suspected.

One result is clearly seen, however: Although binning provides half the standard deviation compared to full resolution, the probability to safely detect a peak signal dropped at every distance. If there would be a gain in signal, one would expect more faint stars from a binned image. This cannot be explained with the density of the stars, as the total number of stars found is small compared to the total amount of Millions of pixel of the sensor surface (the stellar density of the sample is demonstrated in figure 2).

Table 1. Results from the obtained number of stars from a search of local maximum above 3 sigma of the standard deviation. Numbers marked with an asterisk (*) are the minimum distances taken for the binned images of half the size.

Min. distance	Binning of single frame	Co-added image	Co-added & binned
10, 5*	1372	1329	1183
8, 4*	1479	1468	1261
6, 3*	1559	1569	1342
4, 2*	1612	1681	1395
2	-	1795	-

4. EFFICIENT BINNING

The binning task applied to a single raw frame yielded almost the same standard deviation compared to a co-added image of four single images at full resolution. Does it mean to have equal or better signal with binning and compared to full resolution of longer exposures? Is there found a gain of susceptibility of the device? First of all, the co-added result and the binned sample, have a different amount of pixels and spatial resolution. Therefore, a further application of the binning task to the co-added image again improves the standard deviation of the background signal, too. Hence, both results, the binned sample and the co-added long

exposure are impossible to compare this way. A surprising result is: The co-added and binned image yielded less stars from the analysis. An explanation is needed.

4.1 Calculation of the SNR

The expectation value of the number of photo electrons detected is proportional to the expectation value of energy. More energy yield more counts N_{PE} detected and vice versa. The standard deviation of the photo counts is proportional to the square root of the photo count (see equation 3). Having a larger signal-to-noise ratio will also mean a detection of a larger photo count. The binning task provides a way to amplify the flux by decrease of the standard deviation. From the equation 3, a drop of the standard deviation σ_I versus the expectation value $<I(x)>$ must be a change of the quantum conversion factor g_{PC} or the quantum efficiency of the detector changed. The latter would increase the susceptibility of the detector due to transformation of intensity values already measured. Now a virtual quantum efficiency of more than 100% can be created. This means the physical relation is lost. Obviously, a perpetual motion machine producing energy is created, which violates the physical law of conservation of energy. Hence, with the proof by contradiction, the use of PSNR is inappropriate to describe physical properties of the device and signal.

The use of PSNR may lead to certain confusion and wrong conclusions, like having found a gain in susceptibility of the detector, which is not the case. This reflects well the observation of Mullikin et al. (1994). They also found an increase of the peak SNR with no increase of susceptibility of several devices tested. To correct the funny situation, the signal-to-noise ratio shall consider the total flux of a point light source detected by the optics of the camera.

Stars with almost infinite distances appear like the optical point spread function itself, which is caused by diffraction of the optics (Born & Wolf, 1953). (Point spread includes further effects, like atmospheric blur and possible residuals from the telescope movement in this case.) The illumination caused by the point spread is spatially distributed across pixel groups. The binning task averaged these pixel group intensities 2×2. The intensities of sky background and nebula are averaged in the same way. Point spread causes a certain signal degradation as a smear of $N_{PE|A}$ over the two-dimensional surface area of A pixels. The integrated signal $N_{PE|A}$ shall be evaluated from all pixel intensities contained in area A. The area A shall be a squared surface area of width $\sqrt{A}$, which is a multiple of the bin size N. This yields

$$<N_{PE|A}> = \; < \int_{x \in A} N_{PE}(x)\, dx > = \int_{x \in A} <N_{PE}(x)>\, dx = Var(N_{PE|A}).$$

Eq. 6

Binning N×N shrinks A by N^2. Let $1/N^2 \sum_{NxN} N_{PE}(x)$ be the pixel value of the binned signal, A' the surface area obtained by binning task, then the expectation value of the binned signal $N'_{PE|A'}(x)$ is given by:

$$<N'_{PE|A'}> = < \int_{x \in A_\times} 1/N^2 \sum_{NxN} N_{PE}(x)\, dx > = \; Var(\, N'_{PE|A'}\,)$$

Eq. 7

The integral over pixel intensities within areas A and A' define a task of aperture photometry within the original and binned image, respectively. The ratio R between the variances of the original image and the binned image is given by

$$R = Var(N_{PE|A}) / Var(N'_{PE|A'})$$
Eq. 8
$$= Var(\int_{x \in A} N_{PE}(x)\, dx) / Var(\int_{x \in A'} 1/N^2 \sum_{NxN} N_{PE}(x)\, dx) = N^2$$

The computation yields a variance of the binned signal decreased by the factor $1/N^2$. The ratio between the standard deviations computed from the images yields the value N, which is the dimension of the bin. However, the factor N^2 is an arbitrary normalization chosen by the binning task to compute an average of the intensities. If the same calculation is done by summation of the pixel intensities instead of taking the average, the ratio R will yield the value $R=1$. It follows, that the total SNR of the photo events of a point source is constant at all scales, at full resolution and any scale from binning. Hence, the conservation of energy is not violated with binning. The susceptibility of the imaging detector is left untouched. Any decrease of the standard deviation found is caused by an arbitrary normalization. To give an example: With a 2×2 binning task, the pixel dimension of the image is reduced by the factor two. The total amount of photo counts detected within the smaller area of pixels of dimension A decreased by four (due to the division of the average). σ_{PE} is obtained at half the value. On the other hand, the flux is now obtained as one 4th of pixels averaged. The ratio between the signal components and the noise remains the same with any binning scale.

A further note on aperture photometry: With the real photo optics any point spread will occur within an infinite area A. To give an example: The resulting rotational symmetric $sinc^2$ function of the point spread of a circular aperture of a camera optics is defined everywhere in the focal plane of the chip (Born & Wolf, 1953). Therefore, photo events of a single point source are theoretically found everywhere on the imaging sensor with a certain probability. Long-exposure imaging within astronomy confirms this very well. Optical diffraction at the mirror mounts of large telescopes will show extended residuals of the diffraction pattern with large exposure time. These are cross-haired spikes around the bright stars from astrophotography. The probability to detect the extended diffraction pattern increases only with the number of photo events collected. However, and for general use, it is sufficient to reduce the analysis to a certain small portion of the point spread, which contains an almost sufficient part of the light, i.e. an integral probability of 99% or more. The probability is given by the normalized integral of the point spread function.

4.2 On-chip Binning

One noise source of imaging detectors is a fixed-pattern noise found from variations of the pixel response (Gilliland, 1992). Subpixel sensitivity variations like intra-pixel sensitivity and pixel cross talk have been discussed by Piterman & Ninkov (2002) and Estribeau & Magnan (2005). Individual pixels yield different amount of photo electrons from the same flux. Binning N×N yields an average $<I_{N\times N}>$ of the pixels weighted by g_{PC}:

$$<I_{N\times N}> = 1/N^2 \sum_{N\times N} I(x) = 1/N^2 \sum_{N\times N} g_{PC}(x)\, N_{PE}(x)$$
Eq. 8

Because of the local variations g_{PC} becomes a function $g_{PC}(x)$ of the two-dimensional pixel coordinate x. The following equation shall define an approximation of the average $\langle I_{tot} \rangle$:

$$1/N^2 \sum_{N\times N} g_{PC}(x)\, N_{PE}(x) \approx 1/N^2 \langle g_{PC}(x) \rangle \sum_{N\times N} N_{PE}(x)$$

Eq. 9

The left hand side can also be interpreted as the average of $g_{PC}(x)$ with weight $N_{PE}(x)$. The right hand side is the arithmetic average of $N_{PE}(x)$ multiplied by $\langle g_{PC}(x) \rangle$, which is the mean value of the electron conversion rate from the binned pixel. Equality is given only, if $N_{PE}(x)$ or $g_{PC}(x)$ are constant with x. $N_{PE}(x)$ taken constant means a flat illumination of the detector (flatfield). Now the average $\langle g_{PC}(x) \rangle$ can be obtained by a normalization of the flatfield detected. On the other hand, the electron conversion factor $g_{PC}(x)$ can also be obtained by noise analysis according to equation 3. Equation 9, however, defines an approximation which yields different standard deviations from the comparison of averaged mean value and arithmetic mean value. Hence, one shall expect a slight mismatch of the mean values and errors estimated. $\langle g_{PC}(x) \rangle$ cannot be disassembled from on-chip binning. Therefore, on-chip binning is expected to yield different errors and quantum conversion factors from the computation and compared to full resolution imaging.

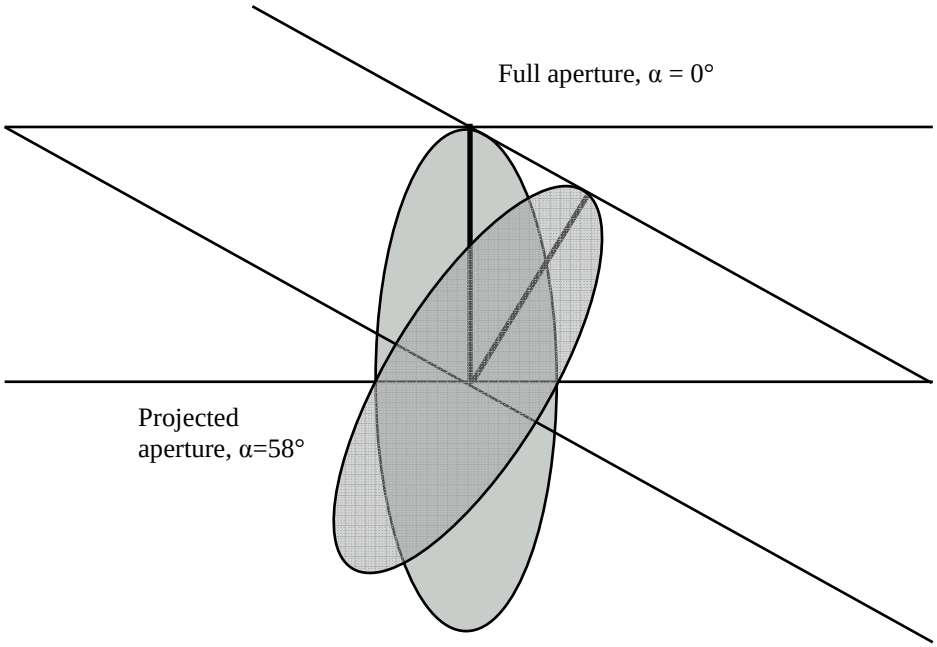

Figure 3. Vignetting reduces the effective aperture, if light falls into the optics with a certain angle. The tilted circle will have the full diameter in one dimension, while the other dimension is decreased from the tilt of the light beam passing the optics. Therefore the effective aperture will be decreased by the cosine of the angle. If both light sources would have the same intensity, the light of the source passing tilted has to be be corrected by division of the cosine to be compared to a light source found with an angle of 0°. The vignetting can also be measured and compensated from flat field exposures.

This situation becomes worse with real optics showing vignetting. If light falls into the optics with a certain angle from the optical axis, the aperture is reduced by the cosine of the angle. This causes a smaller effective aperture. A decrease of illumination to the borders of the image is a consequence. This means, with a real photo optics there is no flat illumination and the calibration of camera and detector becomes complex. As a result of the computation, the tasks of flatfield and binning in principle are not interchangeable tasks. (On the other hand, even with full resolution there remain certain issues with intra-pixel sensitivity.) The amount of calibration and computation of error bars may rise with binning, especially with on-chip binning, if results are compared to imaging at full resolution. Things become worse again with possible non-linearities $g_{PC}(x)$ obtained from the real device. Such problems especially may apply to sensor architectures having dedicated amplifiers with every pixel.

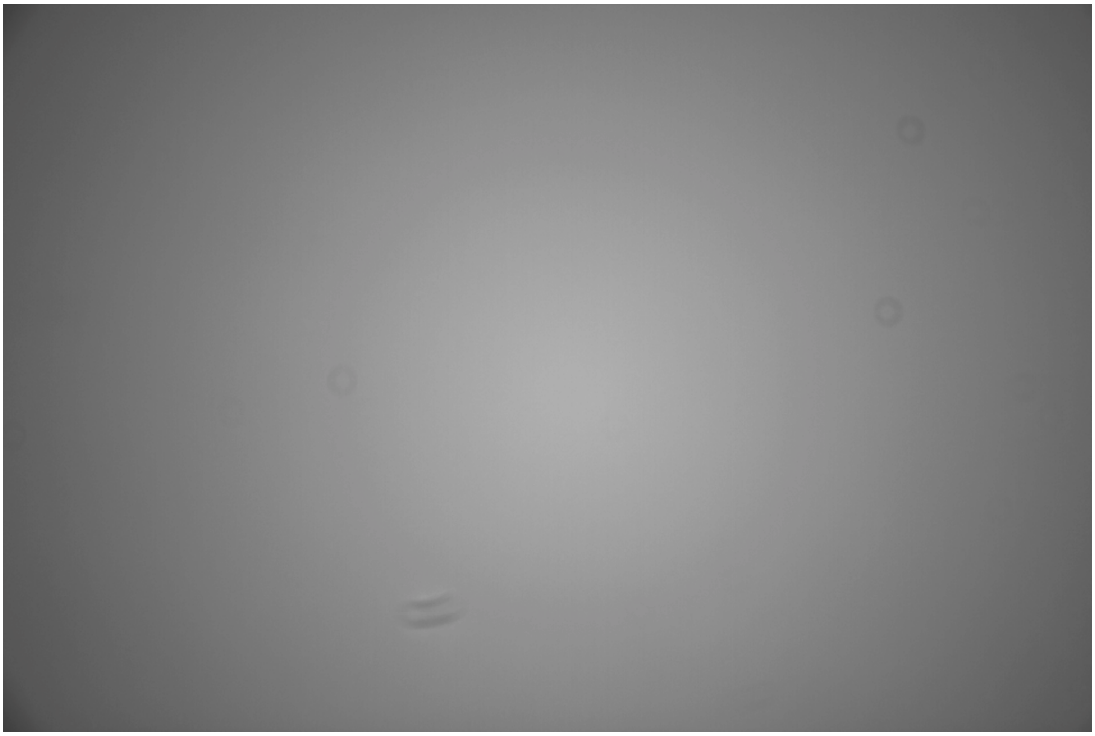

Figure 4. A typical flat field exposure can be taken from the bright sky in daylight or from a flat illuminated wall. With the large focal length of a telescope, it is assumed, that the intensity of the bright sky will not vary within the small angle of view at zenith. The effect of vignetting introduces a certain drop of intensities to the borders of the image. A few „donuts“ are also found in the image and caused by dust. The small particles may be found left in the optics or at the glass plate in front of the imaging sensor. The flat field also represents the local variation of pixel sensitivity. In a first order approximation the variations of sensitivity are be compensated from a division by the flatfield exposure (which should be an averaged flatfield, if statistical image processing is applied).

5. CRITICAL EVALUATION

As shown above, the binning task will not improve the susceptibility of the device. Instead, the use of peak SNR is found inappropriate to describe the physical properties of both, the detector and signal. This is not very surprising, however. A pixel detector is a physical device. A pixel has a geometric dimension and surface, where the flux of light is detected. The image of optical point spread is a surface illumination in any case of imaging, whether it is under-sampled, well sampled, or over-sampled. Binning will mean a change of the image dimension. Therefore, a PSNR will not apply for several reasons. With the above definition of the total signal versus standard deviation, binning will not introduce a change in the SNR of the flux. Instead, the SNR is constant at any scale. This represents well the physical law of conservation of energy. There are a few consequences seen, so far. Binning increases the complexity of computation of signal and errors, when applied to high-precision photometric analysis of a real detector. The exercise of an appropriate calibration method for on-chip binning and computation of errors obtained, is left open, however.

A further issue is seen from the use of PSNR. This is coupled to considerations about optimal sampling (Nyquist, 1928). From the visual comparison of binned samples containing images of point light sources, binning may reach the point where the image starts to get under-sampled. One might expect to have found an optimum peak SNR with a one pixel sampling. This is not true, due to statistical reasons. The extended point spread takes place between pixels. Therefore, a point source falling on a pixel center represents a larger peak compared to the situation, when it falls exactly between four pixels (only a quarter of the peak distributed over four pixels). With the definition of significance coupled to the standard deviation of the image, the probability to loose photometric relevant information rises with the loss of spatial resolution caused by binning.

From theory and experiments follow a few conditions of a successful and meaningful application of the binning task. Binning may apply to correct oversampling. It shall be proven, however, whether the point spread of the camera represents over-sampled images, or not. As binning has been shown not to provide a gain of signal, optimal linear image analysis is found with optimal sampling. To give an example: For a typical digital single lens reflex camera and modern optics, the photo optics is adapted to the typical pixel dimension. There is an exemption: An extended light source might be invisible due to strong scatter within an image (physiological effects). Therefore, it might be possible to demonstrate the existence of such an extended object within the noisy signal with binning. Of course, this will mean a loss of details with no better opportunity to photometry, because the SNR remains the same. The possible danger to smear other objects with the extended source may rise as well. The only way to improve a bad signal is the collection of more photo quants.

The application of binning within image processing is a trade-off and will result in (1) loss of spatial resolution, (2) loss of photometric information, (3) a gain in computation overhead and (4) gain in complexity of linear image calibration - at no further gain in signal. This means, the application of a binning task, either driven by software or hardware, is not an effective choice. The advantage of binning is a smaller storage capacity needed to store any images.

6. CONCLUSION

Pixel binning is a trivial image transformation. However, consequences are non-trivial and seem to contradict common sense. Because the flux of light is spread over a two-dimensional surface area, an appropriate definition of signal versus noise shall take into account the surface *A* of pixel dimensions and point spread. It is shown, that binning yields no increase of signal or increase of the ratio between the signal and noise. This represents the physical law of conservation of energy. Consequently, binning is not a method to improve a bad photography. An improvement of a bad optical signal shall be done by the collection of a larger photo count. Any application of binning shall end at almost optimal pixel sampling of the point spread. There are a few issues found with binning and especially on-chip binning. The determination of the electron conversion factor of a specific device is coupled to considerations of the Poisson statistics of the electron current measured. Binning may introduce a certain complexity to the computation of the quantum efficiency, electron conversion rate and errors. In principle, the tasks to determine the electron conversion rate and pixel response are not interchangeable with the binning task. Therefore on-chip binning applied before the calibration may introduce certain disadvantages over software binning performed after the image calibration. If linear image processing is a strong requirement, binning will introduce a certain inefficiency with the tasks of calibration and image analysis.

REFERENCES

Berry, R. and Burnell, J., 2006. The Handbook of Astronomical Image Processing. 2nd. english ed., Wilmann-Bell, Inc., Richmond, VA, USA

Blakeslee, J. P., et al., 2003. An Automatic Image Reduction Pipeline for the Advanced Camera for Surveys. *Astronomical Data Analysis Software and Systems XII ASP Conference Series, Vol. 295*, 2003 H. E. Payne, R. I. Jedrzejewski, and R. N. Hook, eds.

Born M. and Wolf, E., 1953. Principles of Optics. Pergamon Press, Great Britain, 195

Estribeau, M. and Magan, P., 2005. CMOS pixels crosstalk mapping and its influence on measurements accuracy for space applications. Sensors, Systems, and Next-Generation Satellites IX. Edited by Meynart, R.; Neeck, S. P.; Shimoda, H. Proceedings of the SPIE, Volume 5978, pp. 315-326 (2005)

Fellers, T. J. and Davidson M.W., 2010, Concepts in Digital Imaging Technology, CCD Noise Sources and Signal-to-Noise Ratio. http://learn.hamamatsu.com/articles/ccdsnr.html, visited 2010

Foi, A. et al., 2008. Practical Poissonian-Gaussian noise modeling and fitting for single-image raw-data. IEEE Transactions on Image Processing, vol. 17, issue 10, pp. 1737-1754

Gilliland, R. L., 1992. Details of Noise Sources and Reduction Processes. Astronomical CCD observing and reduction techniques, edited by Steve B. Howell. Published 1992 Astronomical Society of the Pacific, vol. 23 San Francisco, CA. ISBN 0-937707-42-4, LCCN 92-71172, p. 68.

Howell, S. B., 2006. Handbook of CCD Astronomy. Cambridge University Press, second edition, Cambridge, UK.

Mackay, C. D., 1986. Charge-coupled devices in astronomy. *Annual review of astronomy and astrophysics.* Volume 24, A87-26730 10-90). Palo Alto, CA, Annual Reviews, Inc., 1986, p. 255-283

Mullikin, J.C. et al, 1994. Methods for CCD Camera Characterization. *Proc. SPIE*, vol. 2173, 73

Nyquist, H, 1928. Certain topics in telegraph transmission theory. Trans. AIEE, vol. 47, pp. 617-644

Piterman, A. and Ninkov, Z., 2002. Subpixel sensitivity maps for a back-illuminated charge-coupled device and the effects of nonuniform response on measurement. *Optical Engineering,* Vol. 41(06), p. 1192-1202, D. C. O'Shea; Ed.

Planck, M., 1901. On the Law of Distribution of Energy in the Normal Spectrum. *Annalen der Physik.* vol.4, p.553